Finite-size scaling of charge carrier mobility in disordered organic semiconductors

Pascal Kordt,[1,*] Thomas Speck,[2,†] and Denis Andrienko[1,‡]
[1]*Max Planck Institute for Polymer Research, Ackermannweg 10, 55128 Mainz, Germany*
[2]*Institute of Physics, Johannes Gutenberg University, Staudingerweg 7-9, 55128 Mainz, Germany*
(Received 18 June 2015; revised manuscript received 10 June 2016; published 25 July 2016)

Simulations of charge transport in amorphous semiconductors are often performed in microscopically sized systems. As a result, charge carrier mobilities become system-size dependent. We propose a simple method for extrapolating a macroscopic, nondispersive mobility from the system-size dependence of a microscopic one. The method is validated against a temperature-based extrapolation [A. Lukyanov and D. Andrienko, Phys. Rev. B **82**, 193202 (2010)]. In addition, we provide an analytic estimate of system sizes required to perform nondispersive charge transport simulations in systems with finite charge carrier density, derived from a truncated Gaussian distribution. This estimate is not limited to lattice models or specific rate expressions.

DOI: 10.1103/PhysRevB.94.014208

I. INTRODUCTION

Charge carrier mobility is the key characteristic of organic semiconductors. Experimentally, it can be extracted from time-of-flight measurements [1,2], current-voltage characteristics in a diode [3,4] or field-effect transistor [5,6], pulse-radiolysis time-resolved microwave conductivity measurements [7], or other techniques [8–17].

In amorphous organic materials the energetic landscape sampled by a charge carrier can be rather rough, with the width of the density of states as large as 0.2 eV. As a result, charge transport in thin films becomes dispersive; that is, the extracted mobility varies with the film thickness [18–20]. Consequently, the intrinsic value of mobility is difficult to measure: for example, the film thickness has to be large enough in time-of-flight experiments, imposing stringent requirements on the accuracy of measurements of transient currents.

A similar situation is encountered in computer simulations of charge transport in organic semiconductors. Here, both lattice and off-lattice models employ system sizes which are usually much smaller than those used in experimental setups. This leads to an artificial increase in the average charge carrier energy and, as a result, to overestimated values of the charge mobility [21–23]. In fact, there are two reasons for finite-size effects. The first one is the dependence of the percolation threshold on the system size: in small systems the mobility fluctuations can become comparable to the mobility itself and are system-size dependent [24]. Second, the average charge carrier energy increases with decreasing system size, leading to overestimated values of the charge carrier mobility [21]. Here, we will mostly deal with the second effect, which seems to be the dominant contribution to the finite-size scaling.

To overcome the limitations imposed by small system sizes and the resulting energy increase, a method based on a temperature-extrapolation procedure has recently been proposed [21]. Its main idea is to simulate charge transport at a range of elevated temperatures. At high temperatures transport becomes nondispersive, and one can then extract the nondispersive mobility at relevant (lower) temperatures from the mobility-temperature dependence $\mu(T)$. This method relies on the analytical dependence of the mobility on the temperature derived for a one-dimensional system [25] with Gaussian-distributed energies and Marcus rates for charge transfer (see Sec. II), given by

$$\mu(T) = \frac{\mu_0}{T^{\frac{3}{2}}} \exp\left[-\left(\frac{a}{T}\right)^2 - \left(\frac{b}{T}\right)\right]. \tag{1}$$

Note that it is also possible to derive a similar relation using percolation theory [26,27]. In three dimensions μ_0,a, and b are treated as fitting parameters instead of the parameters derived analytically in one dimension. Hence, for three-dimensional transport, Eq. (1) has to be validated for every particular system. It would therefore be useful to have an alternative approach, which does not rely on the *ad hoc* $\mu(T)$ function. This is the first target of our paper: solving the one-dimensional stochastic transport, we derive the system-size scaling of the mobility and benchmark it against the temperature-based extrapolation.

Due to the filling of the energy levels in the tail of the density of states the charge density is known to have a strong impact on the mobility [28–34]. With increasing density the energy per carrier is increased, leading to higher mobilities. On the other hand, in small systems mobilities are artificially increased. One can therefore presume that the error induced by finite-size effects will decrease with increasing charge carrier density. Hence, the second task of this paper is to provide a criterion for the system size required for nondispersive transport simulations at finite charge concentration.

II. METHODS

To perform mobility simulations, we use the Gaussian disorder model [28,35–37]; that is, we assume that molecular sites are arranged on a cubic lattice and that site energies ϵ_i follow a Gaussian distribution, $f(\epsilon) = 1/\sigma\sqrt{2\pi} \times \exp(-\epsilon^2/2\sigma^2)$, where σ denotes the energetic disorder. We assume a mean of zero throughout. We use the Marcus expression for charge transfer rates [38–40],

$$\omega_{ij} = \frac{2\pi}{\hbar} \frac{J_{ij}^2}{\sqrt{4\pi\lambda_{ij}k_\mathrm{B}T}} \exp\left[-\frac{(\Delta\epsilon_{ij} + q\mathbf{F}\cdot\mathbf{r}_{ij} + \lambda_{ij})^2}{4\lambda_{ij}k_\mathrm{B}T}\right] \tag{2}$$

*kordt@mpip-mainz.mpg.de
†thomas.speck@uni-mainz.de
‡denis.andrienko@mpip-mainz.mpg.de

for transitions $j \to i$, where $\Delta\epsilon_{ij} = \epsilon_i - \epsilon_j$ is the site energy difference, q is the charge, $\mathbf{F}$ is an external field, $\mathbf{r}_{ij} = \mathbf{r}_i - \mathbf{r}_j$ is the distance between two sites, λ_{ij} is the reorganization energy, and J_{ij} denotes the electronic coupling. As a simplification, we assume a constant reorganization energy, $\lambda_{ij} = \lambda$; a constant transfer integral, $J_{ij} = J$; and a lattice spacing of $|\mathbf{r}_{ij}| = a$. Further, T is the temperature, and k_B is the Boltzmann constant. The Marcus rates allow us to link the mobility to the chemical composition of organic semiconductors [22,41–45].

Charge-charge interactions are modeled by an exclusion principle [46]; that is, each site can be occupied by only one charge carrier at a time. As a result, the equilibrium site occupation is given by Fermi-Dirac statistics [47],

$$p(\epsilon) = \left[\exp\left(\frac{\epsilon - \epsilon_\mathrm{F}}{k_\mathrm{B}T}\right) + 1\right]^{-1}, \tag{3}$$

where the Fermi energy ϵ_F is implicitly determined by the number of charges in the system through

$$\int_{-\infty}^{\infty} p(\epsilon) f(\epsilon) \mathrm{d}\epsilon = n. \tag{4}$$

Here, n is the charge carrier density, i.e., the number of charges divided by the number of sites. The average energy per charge carrier ϵ_c is then given by

$$\epsilon_\mathrm{c} = \frac{\int_{-\infty}^{\infty} \epsilon\, p(\epsilon) f(\epsilon) \mathrm{d}\epsilon}{\int_{-\infty}^{\infty} p(\epsilon) f(\epsilon) \mathrm{d}\epsilon}. \tag{5}$$

Note that in the limit of zero charge carrier density or for high temperatures the Fermi-Dirac distribution can be approximated by the Boltzmann distribution, $p_\mathrm{B}(\epsilon) = \exp(-\epsilon/k_\mathrm{B}T)$, which yields $\epsilon_\mathrm{c} = -\sigma^2/k_\mathrm{B}T$.

III. SCALING RELATION

A. Derivation

We now derive and test the system-size dependence of the charge carrier mobility $\mu(N)$ in the limit of zero charge carrier density. The derivation is based on the model of a one-dimensional chain of length N with Gaussian-distributed, uncorrelated energies, and hopping taking place only between adjacent sites according to the Marcus rates, Eq. (2). An electric field of strength $F = |\mathbf{F}|$ is applied in the direction of the chain. We will require the mean velocity

$$v_N(F) = (N-1)\langle \tau_N^{-1} \rangle \approx \frac{N-1}{\langle \tau_N \rangle}, \tag{6}$$

where $\langle\cdot\rangle$ denotes the average over the energetic disorder, i.e., $\langle g(\epsilon)\rangle \equiv \int d\epsilon f(\epsilon) g(\epsilon)$. Here, we have approximated the mean rate by the inverse mean first-passage time $\langle \tau_N \rangle$, which can be calculated more readily.

For completeness, we now present a detailed derivation of $\langle \tau_N \rangle$. At steady-state conditions for a given realization of the disorder, the mean first-passage time to traverse the chain starting at $i = 1$ reads [48–51]

$$\tau_N = \sum_{i=1}^{N-1} \sum_{k=1}^{i} \frac{1}{\omega_{i+1,i}} \frac{\omega_{i-1,i}}{\omega_{i,i-1}} \cdots \frac{\omega_{k,k+1}}{\omega_{k+1,k}}. \tag{7}$$

The rates fulfill a detailed balance, $\omega_{ij}/\omega_{ji} = \exp\{-\beta[\epsilon_i - \epsilon_j - f(i-j)]\}$, which leads to

$$\begin{aligned} \prod_{j=k}^{i-1} \frac{\omega_{j,j+1}}{\omega_{j+1,j}} &= e^{-\beta f(i-k)} \exp\left\{\beta \sum_{j=k}^{i-1} (\epsilon_{j+1} - \epsilon_j)\right\} \\ &= e^{-\beta f(i-k) + \beta(\epsilon_i - \epsilon_k)}, \end{aligned} \tag{8}$$

where $f = qFa$ and $\beta = 1/k_\mathrm{B}T$. After shifting $i - k \mapsto k$, this can be rewritten as

$$\tau_N = \sum_{i=1}^{N-1} \frac{1}{\omega_{i+1,i}} \sum_{k=0}^{i-1} e^{-\beta f k + \beta(\epsilon_i - \epsilon_{i-k})}. \tag{9}$$

For Gaussian-distributed energies the exponential e^{ϵ_i} is log-normally distributed with mean $e^{\sigma^2/2}$. Since, furthermore, energies are uncorrelated, $\langle \epsilon_i \epsilon_j \rangle = \sigma^2 \delta_{ij}$, for $k > 0$ we have

$$\langle e^{-\beta\epsilon_{i-k}} \rangle = e^{\frac{1}{2}(\beta\sigma)^2}, \tag{10}$$

leading to

$$\begin{aligned} \langle \tau_N \rangle &= \sum_{i=1}^{N-1} \left\langle \frac{e^{\beta\epsilon_i}}{\omega_{i+1,i}} \right\rangle \left[1 + e^{\frac{1}{2}(\beta\sigma)^2} \sum_{k=1}^{i-1} e^{-\beta f k}\right] \\ &= \sum_{i=1}^{N-1} \left\langle \frac{e^{\beta\epsilon_i}}{\omega_{i+1,i}} \right\rangle \left[1 + e^{\frac{1}{2}(\beta\sigma)^2} \frac{z - z^i}{1 - z}\right] \end{aligned} \tag{11}$$

(geometric series with $z = e^{-\beta f} < 1$). We can split the average because the first term only involves i and $i+1$ and the second term involves sites $<i$. The first term becomes

$$I(f) = \left\langle \frac{e^{\beta\epsilon_i}}{\omega_{i+1,i}} \right\rangle = \frac{1}{\omega_0} \langle e^{\beta\epsilon_i + \beta/(4\lambda)(\epsilon_{i+1} - \epsilon_i + \lambda')^2} \rangle, \tag{12}$$

where $\omega_0 = 2\pi J^2/\hbar\sqrt{4\pi\lambda k_\mathrm{B}T}$ is the prefactor of the rates equation (2) and $\lambda' = \lambda - f$ is the shifted reorganization energy. It is convenient to transform site energies as

$$\epsilon_i = \bar{\epsilon} - \tfrac{1}{2}\delta, \quad \epsilon_{i+1} = \bar{\epsilon} + \tfrac{1}{2}\delta. \tag{13}$$

The brackets above become

$$\begin{aligned} I(f) = \frac{1}{2\pi\sigma^2 w_0} \int \mathrm{d}\bar{\epsilon}\mathrm{d}\delta \exp\Bigg\{ &-\frac{1}{\sigma^2}\bar{\epsilon}^2 - \frac{1}{4\sigma^2}\delta^2 \\ &+ \beta\bar{\epsilon} - \frac{1}{2}\beta\delta + \frac{\beta}{4\lambda}(\delta + \lambda')^2 \Bigg\} \end{aligned} \tag{14}$$

since integrals over other sites reduce to unity and the variable change has unity Jacobian. The integral over $\bar{\epsilon}$ can be evaluated straightforwardly, leading to

$$\begin{aligned} I(f) = \frac{1}{2\sqrt{\pi}\sigma w_0} e^{\frac{1}{4}(\beta\sigma)^2} \int \mathrm{d}\delta \exp\Bigg\{ &-\frac{1}{4\sigma^2}\delta^2 - \frac{1}{2}\beta\delta \\ &+ \frac{\beta}{4\lambda}(\delta + \lambda')^2 \Bigg\}. \end{aligned} \tag{15}$$

Evaluating the second integral, we have

$$\begin{aligned} I(f) = \frac{\tilde{\sigma}}{w_0\sigma} \exp\Bigg\{ &\frac{1}{4}(\beta\sigma)^2 + \frac{1}{2}(\beta\tilde{\sigma})^2 \frac{f^2}{\lambda^2} \\ &+ \frac{1}{4}\beta\lambda\left(1 - \frac{f}{\lambda}\right)^2 \Bigg\}, \end{aligned} \tag{16}$$

with

$$\frac{1}{\tilde{\sigma}^2} = \frac{1}{\sigma^2} - \frac{\beta}{\lambda}, \qquad \tilde{\sigma}^2 = \frac{\lambda\sigma^2}{\lambda - \beta\sigma^2} = \frac{\sigma^2}{1 - \beta\sigma^2/\lambda}. \quad (17)$$

Note that this result implies, in principle, an upper bound $(\beta\sigma)^2 < \beta\lambda$ for the disorder σ, beyond which the mean waiting time diverges and, consequently, the approximation in Eq. (6) breaks down. The mean waiting time finally reads

$$\langle \tau_N \rangle = I(f) \sum_{i=1}^{N-1} \left[1 + e^{\frac{1}{2}(\beta\sigma)^2} \frac{z - z^i}{1 - z} \right], \quad (18)$$

which constitutes our first central result.

B. Mobility

We first consider the limit $z \to 1$ corresponding to a vanishing field, $F \to 0$, before evaluating the sum. We thus obtain

$$\begin{aligned} \langle \tau_N \rangle &= I(0) \sum_{i=1}^{N-1} \left[1 + e^{\frac{1}{2}(\beta\sigma)^2} (i - 1) \right] \\ &= I(0)(N-1) \left[1 + e^{\frac{1}{2}(\beta\sigma)^2} \left(\frac{N}{2} - 1 \right) \right] \end{aligned} \quad (19)$$

using

$$\lim_{z \to 1} \frac{z - z^i}{1 - z} = i - 1. \quad (20)$$

For large N,

$$\langle \tau_N \rangle \approx I(0) e^{\frac{1}{2}(\beta\sigma)^2} \frac{N}{2} (N - 1), \quad (21)$$

and the velocity decays as $v_N(0) \sim 1/N$. On the other hand, evaluating the sum first, we obtain

$$\langle \tau_N \rangle = I(f) \left[(N-1) + e^{\frac{1}{2}(\beta\sigma)^2} \frac{(N-1)z(1-z) - (z - z^N)}{(1-z)^2} \right], \quad (22)$$

which reduces to the same result as Eq. (21) in the limit $z \to 1$ applying L'Hôpital's rule twice.

For a finite field, by putting Eq. (22) into Eq. (6) and taking the limit $N \to \infty$, we get

$$\frac{1}{v_\infty} = I(f) \left(1 + e^{\frac{1}{2}(\beta\sigma)^2} \frac{z}{1 - z} \right) \approx I e^{\frac{1}{2}(\beta\sigma)^2} \frac{z}{1 - z}. \quad (23)$$

With a few simplifications for sufficiently large N, we can thus write

$$\frac{1}{v_N} \approx \frac{1}{v_\infty} \left(1 - \frac{1}{N} \frac{1}{1 - z} \right). \quad (24)$$

To leading order this results in

$$v_N \approx v_\infty \left(1 + \frac{1}{N} \frac{1}{1 - z} \right) > v_\infty. \quad (25)$$

Specifically, for the zero-field mobility we obtain

$$\mu_\infty = \left. \frac{\partial v_\infty}{\partial f} \right|_{f=0} = \frac{\beta w_0 \sigma}{\tilde{\sigma}} \exp \left\{ -\frac{3}{4}(\beta\sigma)^2 - \frac{1}{4}\beta\lambda \right\}, \quad (26)$$

which is the same result that Seki and Tachiya [25] obtained in their Eq. (6.7) [see Eq. (1)]. Going beyond their result and including the leading-order correction, we find for the mobility of the one-dimensional chain of N sites

$$\mu_N = \mu_\infty \left(1 + \frac{c}{N} \right), \quad (27)$$

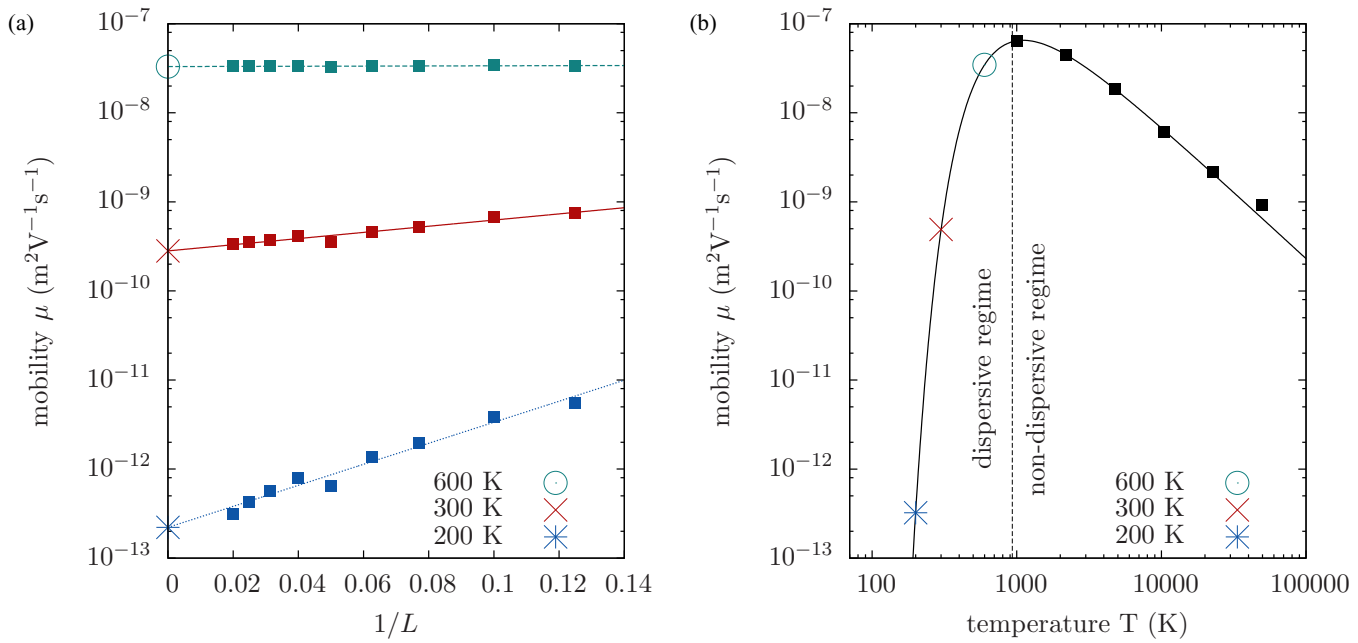

FIG. 1. (a) System-size extrapolation for energetic disorder of $\sigma = 0.1\,eV$, external field of $F = 10^6\,V/m$, lattice spacing of 1 nm, transfer integral of $J = 10^{-3}\,eV$, and reorganization energy of $\lambda = 0.3\,eV$. (b) Validation using the temperature extrapolation. Large symbols denote the extrapolated mobilities μ_∞, summarized in Table I.

with $c = \frac{3}{2}$. For large N this result can be further simplified to $\ln \mu_N \approx \ln \mu_\infty + \frac{c}{N}$.

C. Numerical test

Like for the temperature-based extrapolation, we now assume that Eq. (27) also holds in three dimensions, but with a different constant c. The dependence on the number of sites is replaced by a dependence on the box length, $L = N^{1/3}$, in three dimensions. To test this assumption and to extrapolate the mobility value, we performed kinetic Monte Carlo simulations in cubic lattices from $8 \times 8 \times 8$ to $50 \times 50 \times 50$ sites, with Gaussian-distributed energies and Marcus rates as described in Sec. II. The master equation for occupation probabilities is solved using the variable-step-size Monte Carlo algorithm [23,52,53]. The charge mobility, $\mu = d/\tau F$, is evaluated using the charge trajectory, where d is the distance traveled by the charge along the field F during time τ. Results are shown in Fig. 1(a). One can see that the mobility (and its logarithm) scales indeed linearly with the inverse box length.

The extrapolated mobilities, $\mu_\infty = \mu(N \to \infty)$, also agree well with the temperature-based extrapolation, which is shown in Fig. 1(b). Both methods are compared in more detail in Table I.

IV. FINITE CARRIER DENSITY

We now turn to the estimation of the error introduced by finite-size effects in systems with finite charge carrier density. A generalization of the approach of Sec. III to multiple interacting carriers is not straightforward since we are now faced with an exclusion process in the presence of disorder, for which an analytical result for the mean first-passage time is not available. Instead, we use the average energy per carrier $\epsilon_c(N)$ as a figure of merit. This also makes the error estimate independent of the rate expression and the positional order of sites. Hence, it is also applicable to realistic morphologies and models with different charge transfer rates.

We first perform a direct evaluation of $\epsilon_c(N)$ by drawing N random energies ϵ_i from a Gaussian distribution of width σ and calculating the ensemble average as

$$\epsilon_c(N) = \frac{\sum_{i=1}^{N} \epsilon_i \, p(\epsilon_i)}{\sum_{i=1}^{N} p(\epsilon_i)}. \tag{28}$$

Results for $\sigma = 0.1$ eV and $T = 300$ K are shown in Fig. 2 (symbols) for different charge densities. This demonstrates that in finite systems there is a significant deviation from ϵ_c, especially at low charge carrier densities.

In order to obtain a closed-form expression for the finite-size error, we first note that the probability to draw an energy

TABLE I. Extrapolated mobilities for the thermodynamic limit μ_∞ from the temperature extrapolation method and the system-size extrapolation method (in $m^2\,V^{-1}\,s^{-1}$).

	T extrapolation	N extrapolation
200 K	3.2×10^{-13}	2.2×10^{-13}
300 K	4.9×10^{-10}	2.8×10^{-10}
600 K	3.5×10^{-8}	3.3×10^{-8}

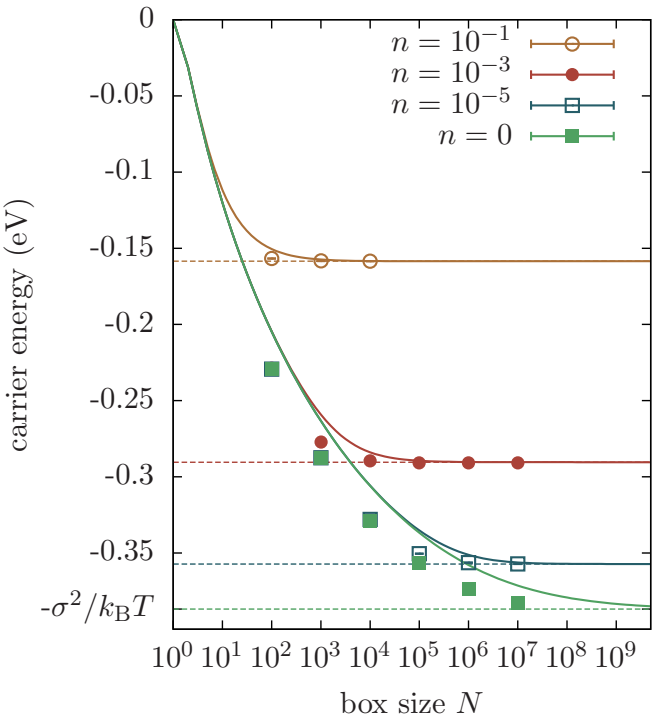

FIG. 2. Convergence of the carrier energy with system size N for different carrier densities n. Symbols are the results of random-number experiments, Eq. (28), while solid lines are the predictions of our analytic model, Eq. (35). The dashed lines are the exact values for ϵ_c as $N \to \infty$ obtained from Eq. (5).

smaller than ϵ_0 from a Gaussian distribution $f(x)$ reads

$$\mathcal{P}(\epsilon \leqslant \epsilon_0) = \int_{-\infty}^{\epsilon_0} f(x)\mathrm{d}x = F(\epsilon_0), \tag{29}$$

where $F(x)$ is the cumulative distribution function

$$F(x) = \frac{1}{2} + \frac{1}{2}\mathrm{erf}\left(\frac{x}{\sqrt{2\sigma^2}}\right). \tag{30}$$

The probability to draw an energy larger than ϵ_0 is then given by $\mathcal{P}(\epsilon > \epsilon_0) = 1 - F(\epsilon_0)$. If we draw N independent energies, the probability that none of them will be smaller than ϵ_0 reads

$$\mathcal{P}(\epsilon_i > \epsilon_0, i = 1, \ldots, N) = [1 - F(\epsilon_0)]^N. \tag{31}$$

The probability to find one value $\epsilon \leqslant \epsilon_0$ is then given by

$$\begin{aligned}\mathcal{P}(\exists\, i : \epsilon_i \leqslant \epsilon_0) &= 1 - \mathcal{P}(\epsilon_i > \epsilon_0, i = 1, \ldots, N) \\ &= 1 - [1 - F(\epsilon_0)]^N,\end{aligned} \tag{32}$$

which is the cumulative distribution function for ϵ_0. The respective probability distribution for the minimum sampled value (MSV) function is obtained by differentiation and reads

$$f_{\mathrm{MSV}}(x) = -N[F(x)]^{N-1} f(x). \tag{33}$$

We now assume that in a sample of finite size the site energy distribution is given by a truncated Gaussian distribution. The lower cutoff $\epsilon_{\min}$ is the expectation value for the minimum energy, obtained when drawing N energies,

$$\epsilon_{\min} = \int_{-\infty}^{\infty} x \, f_{\mathrm{MSV}}(x)\mathrm{d}x. \tag{34}$$

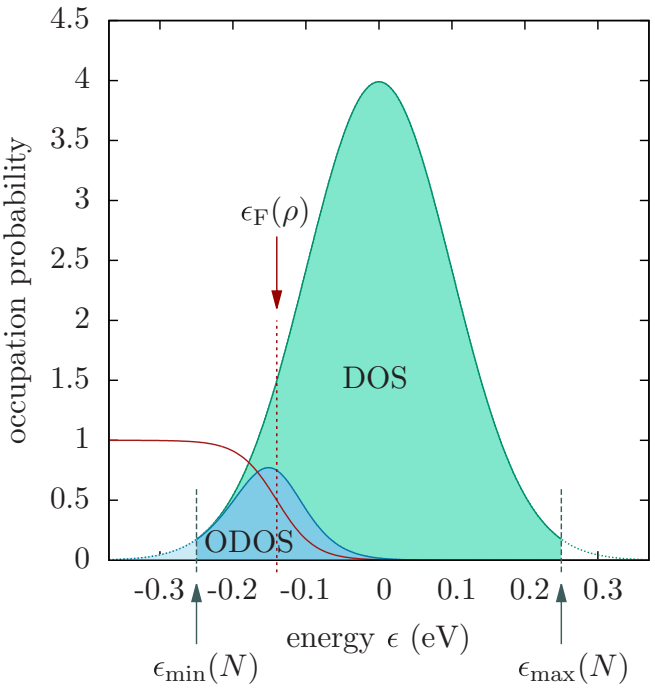

FIG. 3. The occupational density of states (ODOS) is the product of the Gaussian density of states (DOS) and the Fermi-Dirac distribution (red). For finite systems the DOS is approximated by a truncated Gaussian distribution. The light blue part is the missing contribution to the ODOS in a finite system, leading to increased energy values. An increase of the Fermi energy (larger density) or a decrease of $\epsilon_{min}(N)$ (larger box size) reduces this part and thus the finite-size error.

The expectation value for the maximum sampled energy is given by $\epsilon_{max} = -\epsilon_{min}$. With this model distribution function we obtain an estimate for the size-dependent average energy,

$$\epsilon_c(N) \simeq \frac{\int_{\epsilon_{min}}^{\epsilon_{max}} \epsilon\, p(\epsilon) f(\epsilon) \mathrm{d}\epsilon}{\int_{\epsilon_{min}}^{\epsilon_{max}} p(\epsilon) f(\epsilon) \mathrm{d}\epsilon}, \tag{35}$$

which constitutes our second central result. This estimate is also shown in Fig. 2 (solid lines) and is in good agreement with the values simulated directly. Figure 3 illustrates how the cutoff leads to a finite-size error.

Hence, given the error, $\delta\epsilon_c(n,\sigma,N) = |\epsilon_c(n,\sigma,N) - \epsilon_c(n,\sigma,N\to\infty)|$, we can estimate the necessary system size N for our simulations. Such estimates are shown in Table II. As we have anticipated, large energetic disorder requires large system sizes, while for large charge densities one can use smaller systems.

As of today, atomistically resolved simulations can handle systems of approximately 5000 molecules. With coarse-grained models one can increase this number to about 10^6 molecules [23]. In lattice models system sizes are up to 3×10^6 sites [54]. Comparing this to Table II shows that for low carrier densities and for large values of energetic disorder, the necessary system size is computationally still inaccessible, be it a microscopic, stochastic, or lattice model, and the extrapolation schemes from the previous section have to be used. For a sufficiently large charge carrier density or small energetic disorder, however, the error is within an acceptable range even for simulations in smaller systems.

TABLE II. Necessary system size (order of magnitude) for different values of energetic disorder σ and charge carrier density n to ensure that the relative error on the energy per charge carrier, $\delta\epsilon_c/\epsilon_c$, is smaller than 5% and 0.1%, assuming a temperature of 300 K. Errors are calculated using the difference of the analytic estimate, Eq. (35), to the exact value in an infinite system, Eq. (5).

	$\delta\epsilon_c/\lvert\epsilon_c\rvert \leqslant 5\%$			$\delta\epsilon_c/\lvert\epsilon_c\rvert \leqslant 0.1\%$		
$n \backslash \sigma$(eV)	0.001	0.01	0.1	0.001	0.01	0.1
0	10^3	10^3	10^7	10^5	10^5	$>10^{10}$
10^{-7}	10^3	10^3	10^7	10^5	10^5	10^{10}
10^{-6}	10^3	10^3	10^6	10^5	10^5	10^9
10^{-5}	10^3	10^3	10^6	10^5	10^5	10^8
10^{-4}	10^3	10^3	10^5	10^5	10^5	10^7
10^{-3}	10^3	10^3	10^4	10^5	10^5	10^6
10^{-2}	10^3	10^3	10^3	10^5	10^5	10^5
10^{-1}	10^3	10^3	10^3	10^5	10^5	10^3

V. CONCLUSIONS

To conclude, we have derived a system-size dependence of charge carrier mobility and provided a simple way of correcting for finite-size effects in computer simulations of charge transport in disordered organic semiconductors. We have also estimated the system sizes required for simulating charge transport of carriers with a given energetic disorder in the density of states. Our results are general and are applicable to different rate expressions as well as off-lattice morphologies.

ACKNOWLEDGMENTS

This work was partially supported by Deutsche Forschungsgemeinschaft (DFG) under the Priority Program "Elementary Processes of Organic Photovoltaics" (SPP 1355) and the program IRTG 1404, by BMBF grants MESOMERIE (FKZ 13N10723) and MEDOS (FKZ 03EK3503B) and by the European Research Council (ERC) NMP-20-2014 - "Widening materials models" program under Grant Agreement No. 646259 (MOSTOPHOS). We are grateful to J. Wehner and C. Scherer for a critical reading of the manuscript.

[1] R. G. Kepler, P. M. Beeson, S. J. Jacobs, R. A. Anderson, M. B. Sinclair, V. S. Valencia, and P. A. Cahill, Appl. Phys. Lett. **66**, 3618 (1995).

[2] A. Pivrikas, N. S. Sariciftci, G. Juška, and R. Österbacka, Prog. Photovoltaics **15**, 677 (2007).

[3] P. W. M. Blom, M. J. M. de Jong, and J. J. M. Vleggaar, Appl. Phys. Lett. **68**, 3308 (1996).

[4] A. J. Campbell, D. D. C. Bradley, and D. G. Lidzey, J. Appl. Phys. **82**, 6326 (1997).

[5] O. D. Jurchescu, in *Handbook of Organic Materials for Optical and (Opto)electronic Devices*, edited by O. Ostroverkhova, Woodhead Publishing Series in Electronic and Optical Materials (Woodhead Publishing, Oxford, Cambridge, 2013), pp. 377–397.

[6] Y. Xu, M. Benwadih, R. Gwoziecki, R. Coppard, T. Minari, C. Liu, K. Tsukagoshi, J. Chroboczek, F. Balestra, and G. Ghibaudo, J. Appl. Phys. **110**, 104513 (2011).

[7] A. M. van de Craats, J. M. Warman, M. P. de Haas, D. Adam, J. Simmerer, D. Haarer, and P. Schuhmacher, Adv. Mater. **8**, 823 (1996).

[8] J. Fischer, W. Tress, H. Kleemann, J. Widmer, K. Leo, and M. Riede, Org. Electron. **15**, 2428 (2014).

[9] J. Widmer, J. Fischer, W. Tress, K. Leo, and M. Riede, Org. Electron. **14**, 3460 (2013).

[10] I. P. Batra, J. Appl. Phys. **41**, 3416 (1970).

[11] C. Hosokawa, H. Tokailin, H. Higashi, and T. Kusumoto, Appl. Phys. Lett. **60**, 1220 (1992).

[12] D. Moses and A. J. Heeger, J. Phys. Condens. Matter **1**, 7395 (1989).

[13] W. Brütting, P. H. Nguyen, W. Rieß, and G. Paasch, Phys. Rev. B **51**, 9533 (1995).

[14] J. Cabanillas-Gonzalez, T. Virgili, A. Gambetta, G. Lanzani, T. D. Anthopoulos, and D. M. de Leeuw, Phys. Rev. Lett. **96**, 106601 (2006).

[15] G. Juška, K. Arlauskas, M. Viliūnas, and J. Kočka, Phys. Rev. Lett. **84**, 4946 (2000).

[16] N. Karl, K.-H. Kraft, and J. Marktanner, Synth. Met. **109**, 181 (2000).

[17] H. C. F. Martens, J. N. Huiberts, and P. W. M. Blom, Appl. Phys. Lett. **77**, 1852 (2000).

[18] V. R. Nikitenko and H. v. Seggern, J. Appl. Phys. **102**, 103708 (2007).

[19] F. Laquai, G. Wegner, C. Im, H. Bässler, and S. Heun, J. Appl. Phys. **99**, 033710 (2006).

[20] T. Kreouzis, D. Poplavskyy, S. M. Tuladhar, M. Campoy-Quiles, J. Nelson, A. J. Campbell, and D. D. C. Bradley, Phys. Rev. B **73**, 235201 (2006).

[21] A. Lukyanov and D. Andrienko, Phys. Rev. B **82**, 193202 (2010).

[22] P. Kordt, O. Stenzel, B. Baumeier, V. Schmidt, and D. Andrienko, J. Chem. Theory Comput. **10**, 2508 (2014).

[23] P. Kordt, J. J. M. van der Holst, M. Al Helwi, W. Kowalsky, F. May, A. Badinski, C. Lennartz, and D. Andrienko, Adv. Funct. Mater. **25**, 1955 (2015).

[24] A. Massé, R. Coehoorn, and P. A. Bobbert, Phys. Rev. Lett. **113**, 116604 (2014).

[25] K. Seki and M. Tachiya, Phys. Rev. B **65**, 014305 (2001).

[26] J. Cottaar, L. J. A. Koster, R. Coehoorn, and P. A. Bobbert, Phys. Rev. Lett. **107**, 136601 (2011).

[27] The resulting equation has the same temperature dependence as Eq. (1), but with a different exponent in the power law (0.15 instead of 3/2 for a simple cubic lattice with Marcus rates). In our simulations the one-dimensional expression agrees better with simulation results.

[28] W. F. Pasveer, J. Cottaar, C. Tanase, R. Coehoorn, P. A. Bobbert, P. W. M. Blom, D. M. de Leeuw, and M. A. J. Michels, Phys. Rev. Lett. **94**, 206601 (2005).

[29] V. I. Arkhipov, E. V. Emelianova, P. Heremans, and H. Bässler, Phys. Rev. B **72**, 235202 (2005).

[30] S. D. Baranovskii, O. Rubel, and P. Thomas, J. Non-Cryst. Solids **352**, 1644 (2006).

[31] O. Rubel, S. D. Baranovskii, P. Thomas, and S. Yamasaki, Phys. Rev. B **69**, 014206 (2004).

[32] J. J. Brondijk, F. Maddalena, K. Asadi, H. J. van Leijen, M. Heeney, P. W. M. Blom, and D. M. de Leeuw, Phys. Status Solidi B **249**, 138 (2012).

[33] C. Tanase, P. W. M. Blom, D. M. de Leeuw, and E. J. Meijer, Phys. Status Solidi A **201**, 1236 (2004).

[34] C. Tanase, E. J. Meijer, P. W. M. Blom, and D. M. de Leeuw, Phys. Rev. Lett. **91**, 216601 (2003).

[35] H. Bässler, Phys. Status Solidi B **175**, 15 (1993).

[36] M. Bouhassoune, S. v. Mensfoort, P. Bobbert, and R. Coehoorn, Org. Electron. **10**, 437 (2009).

[37] S. V. Novikov, D. H. Dunlap, V. M. Kenkre, P. E. Parris, and A. V. Vannikov, Phys. Rev. Lett. **81**, 4472 (1998).

[38] R. A. Marcus, Rev. Mod. Phys. **65**, 599 (1993).

[39] G. R. Hutchison, M. A. Ratner, and T. J. Marks, J. Am. Chem. Soc. **127**, 2339 (2005).

[40] I. I. Fishchuk, A. Kadashchuk, H. Bässler, and S. Nešpurek, Phys. Rev. B **67**, 224303 (2003).

[41] J. Nelson, J. J. Kwiatkowski, J. Kirkpatrick, and J. M. Frost, Acc. Chem. Res. **42**, 1768 (2009).

[42] V. Rühle, A. Lukyanov, F. May, M. Schrader, T. Vehoff, J. Kirkpatrick, B. Baumeier, and D. Andrienko, J. Chem. Theory. Comput. **7**, 3335 (2011).

[43] F. May, B. Baumeier, C. Lennartz, and D. Andrienko, Phys. Rev. Lett. **109**, 136401 (2012).

[44] J. L. Brédas, J. P. Calbert, D. A. d. S. Filho, and J. Cornil, Proc. Natl. Acad. Sci. USA **99**, 5804 (2002).

[45] Y. Olivier, D. Niedzialek, V. Lemaur, W. Pisula, K. Müllen, U. Koldemir, J. R. Reynolds, R. Lazzaroni, J. Cornil, and D. Beljonne, Adv. Mater. **26**, 2119 (2014).

[46] A more elaborate model of Coulomb interaction than the exclusion principle would lead to small deviations from Fermi-Dirac statistics [55] but is not taken into account here.

[47] G. Kaniadakis and P. Quarati, Phys. Rev. E **48**, 4263 (1993).

[48] N. G. van Kampen, *Stochastic Processes in Physics and Chemistry*, North-Holland Personal Library (North-Holland, Amsterdam, New York, 1992).

[49] K. P. N. Murthy and K. W. Kehr, Phys. Rev. A **40**, 2082 (1989).

[50] K. P. N. Murthy and K. W. Kehr, Phys. Rev. A **41**, 1160 (1990).

[51] G. H. Weiss, Adv. Chem. Phys. **13**, 1 (1967).

[52] K. A. Fichthorn and W. H. Weinberg, J. Chem. Phys. **95**, 1090 (1991).

[53] A. Jansen, Comput. Phys. Commun. **86**, 1 (1995).

[54] J. Cottaar and P. A. Bobbert, Phys. Rev. B **74**, 115204 (2006).

[55] N. Martzel and C. Aslangul, J. Phys. A **34**, 11225 (2001).